

A NEW APPROACH TO CONTROL DIABETES BY CONVERTING EXCESS BLOOD SUGAR TO ENERGY OVER ELECTROCATALYTIC METALLIC ANODE

Subir PAUL¹, Arnab DUTTA*

¹Department of Metallurgical and Material Engineering,
Jadavpur University, 188, Raja S.C. Mallick Rd, Kolkata 700032, West Bengal, India

Abstract

Diabetes Mellitus, or Diabetes in short, is a group of widespread endocrine diseases characterized by high blood sugar levels. This research paper attempts to find a solution to this high sugar problem, by taking the route of electrochemistry. It was attempted to demonstrate that the excess sugar (glucose) in the bloodstream of a diabetic patient can be lowered by electro-oxidizing the excess sugar in Simulated Body Fluid (SBF) and convert it into electrical energy. For this, a sugar level detection system was developed, using a linear regression model with a coefficient of determination (R^2 value) of 0.974. At first, one of the most popular as well as costly electrocatalytic materials i.e., Platinum was used to electro-oxidize the excess sugar. Upon its success, some highly electrocatalytic but cheap electrode materials were developed, such as Nickel, Nickel with nanocarbon, Manganese dioxide (MnO_2) and Manganese dioxide with nanocarbon (MnO_2/C). And they also successfully electro-oxidized the excess glucose in SBF solution, thereby reducing the sugar levels. Thus, a potentially novel route to deal with the epidemic problem of diabetes has been proposed through this research work.

Keywords: *Electro-oxidation, Material Characterization, Redox Process, Glucose Detection, Diabetes*

Introduction

Diabetes, a chronic metabolic disorder, continues to pose a significant global health challenge, affecting millions of individuals worldwide. It is a group of widespread endocrine diseases characterized by sustained high blood sugar levels [1-2]. The prevalence of diabetes has reached epidemic proportions, with both developed and developing countries experiencing a dramatic increase in cases. Untreated or poorly treated diabetes accounts for approximately 1.5 million deaths per year.

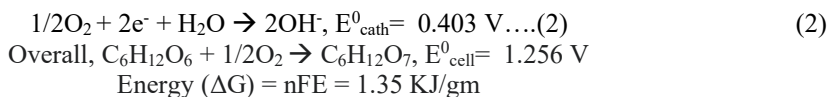
Diabetes can happen either due to the non-production of sufficient insulin by pancreas, or if the body cells do not properly respond to the insulin produced [4]. If diabetes is left untreated, it may cause quite a few health complications [3]. Every year, approximately 1.5 million deaths happen due to non-treatment or poor treatment of diabetes [1]. This qualifies Diabetes to be an epidemic-level disease. Such a situation calls for a novel and alternative route to deal with this epidemic problem, for patients worldwide.

Glucose Fuel Cell

The technology of fuel cell involves the production of electrical energy, from chemical energy [5] using molecules containing high amounts of energy, for example glucose. A glucose fuel cell (GFC) is a fuel cell that relies on oxidation of glucose and reduction of oxygen, in order to

*Corresponding author: mecharnab@gmail.com

produce electricity. A lot of endeavours have been made for developing non Platinum based metals that are inexpensive, alloys and oxides, that can be used as electrocatalytic anode materials in batteries and fuel cells [6-13]. A Glucose fuel cell (GFC) contains two electrocatalytic electrodes: at the cathode, oxygen reduction takes place by electrocatalytic processes while the anode oxidizes glucose.



Equation (1) represents the chemical reaction taking place at the anode. Equation (2) represents the chemical reaction taking place at the cathode. The overall equation of the cell is obtained by summing up the two equations, and it tells that 1.35KJ of electrical energy is obtained by electro-oxidizing 1 gram of glucose [14-15]. In the process of electro-oxidizing the glucose molecules to gluconolactone, the concentration of glucose reduces in the electrochemical cell. This phenomenon forms the basis of the sugar level lowering mechanism, which has been implemented in this research work.

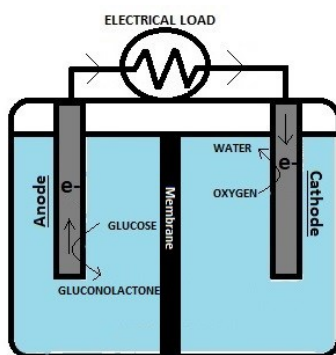


Fig. 1. Schematics of Glucose Fuel Cell

Electro-oxidation of glucose by Platinum

A lot of work has been done towards investigating the direct electro-oxidation of glucose by platinum electrodes [16]. The behaviour of glucose at a platinum electrode in acid, neutral [16] and alkali [16] conditions has been explored by researchers. Different authors have found a similar finding, that gluconolactone is the sole product of glucose oxidation. Gluconolactone hydrolyses to gluconic acid on standing, irrespective of the pH of the solution [16].

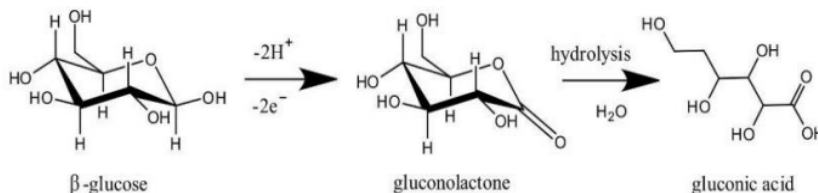


Fig. 2. Oxidation of glucose to gluconolactone and further hydrolysis to gluconic acid

However, spectrochemical evidence suggests other oxidation products such as reduced CO₂, CO_{ads} and fragments of glucose molecule also be present. The cyclic voltammetry (CV) of glucose over platinum electrode shows the three distinct areas, though depending on temperature and electrolyte conditions, it may vary significantly. Investigations by Vasil'ev *et al* [16] highlight the presence of three oxidation peaks, in the anodic sweep.

Electrochemical Glucose Detection –Historical Overview

The first enzyme electrode and amperometric enzymatic biosensors for glucose detection were developed by Clark and Updike, in the 1960s. Glucose oxidase (GOx) based electrochemical glucose sensors have since been studied widely, because of their high specificity, sensitivity, and low detection limit [17]. The catalytic principle of the natural mediator (*i.e.*, oxygen) was used for preparing the first generation of glucose biosensors. The oxygen consumption was followed by electrochemical reduction over an electrode, which was mostly platinum. The cell current increases with the concentration of oxygen and this forms the basis of current measurement. The glucose concentration is then proportional to the current increase. With the second-generation glucose biosensors, the manmade mediators were doped into the enzyme membrane, which can decrease the interference of ambient oxygen [18]. The third generation of glucose biosensors involves direct electron transfer between the enzyme and the electrode without mediators. Using new electrode materials, such as organic conducting salt and conducting organic substances, the electrode can perform direct electron transfer. Ultimately, this glucose biosensors of the third generation would lead to needle-type devices that are implantable. These biosensors can be useful for continuously monitoring of blood glucose, *in vivo* [19]. The fourth-generation glucose sensors include the non-enzymatic sensors, for analytical applications. The flaws of the previous-generation glucose sensors were largely corrected by these non enzymatic biosensors that were first investigated by Walther Loeb, a century ago [20]. For example, a glucose biosensor based on MnO₂/MWNTs composite was fabricated [21], which showed a linear dependence (R = 0.995) in the glucose concentration range up to 28 mM, having a sensitivity of 33.19 μA /mM and a significantly lower overvoltage. In another research work, a glucose sensor based on polyaniline-bimetallic oxide (PANI-MnBaO₂) was reported, which had a limit of detection of 0.06 μM in the concentration range of 0.05 μM–1.6 mM [22].

Experimental

Simulated Body Fluid (SBF)

The solution that closely resembles the ion concentration of blood, that has been used in this experiment, is the Phosphate Buffer Solution (PBS) of pH 7.4. PBS solution is actually a valuable buffer solution because it has similar osmolarity, ion concentrations and pH value of body fluids [23].

Table 1. Ingredients for making PBS solution

Ingredients	Weight/Volume	Final Concentration
Sodium chloride(NaCl)	8.00 grams	137 mM
Potassium chloride(KCl)	0.20 grams	2.7 mM
Disodium phosphate (Na ₂ HPO ₄)	1.44 grams	10 mM
Monopotassium phosphate (KH ₂ PO ₄)	0.24 grams	1.8 mM
Double Distilled water	Up to 1 L	

The different electrocatalytic materials developed in this research work are 1) Nickel 2) Nickel with nanocarbon 3) Manganese dioxide (MnO₂) and 4) Manganese dioxide with

nanocarbon (MnO₂C). All these materials have been developed by the process of electrodeposition, over a Stainless Steel (SS) substrate.

Development of Electrocatalytic Materials

Ni and Ni with Nanocarbon- Stainless steel (SS) samples were first polished by of emery papers of range 2/0 to 3/0. Then the samples were cleaned with water and oxalic acid. Then the samples were dried at the normal room temperature. The steel sample was coated or electrodeposited in the electrolyte solution at 60°C using a DC power source. The current density applied during the process was 300 mA/cm². The sample with Nickel coating was then rinsed in water. Next, it was left overnight at the normal room temperature. The coated sample was then cleaned, first with acetone and after that with ethanol. For Ni-nanocarbon(graphene) electrodeposition, the steel sample was electrodeposited in the same electrolyte solution mixed with graphene powder at 60°C in a DC galvanostatic circuit, using a current density of 300 mA/cm². The electrolyte solution was continuously stirred at 180 rpm, during the electrodeposition process. All the electrodeposition parameters for the synthesis of Ni and NiC materials are tabulated in the below table.

Table 2. Showing the electrodeposition parameters for development of Ni and NiC electrocatalytic materials

Electroplating Parameters	Optimum Value (Ni)	Optimum Value (NiC)
NiCl ₂ : M	0.65	0.65
NiSO ₄ : M	0.30	0.30
H ₃ BO ₃ : M	0.90	0.90
Nano carbon Powder : g/50ml	-----	2
CH ₃ (CH) ₁₁ OSO ₃ Na : gm/lt	1.5	1.5
Applied Current Density: mA/cm ²	250	300
Applied Potential : V	5	3.5
Time duration : minutes	8	12

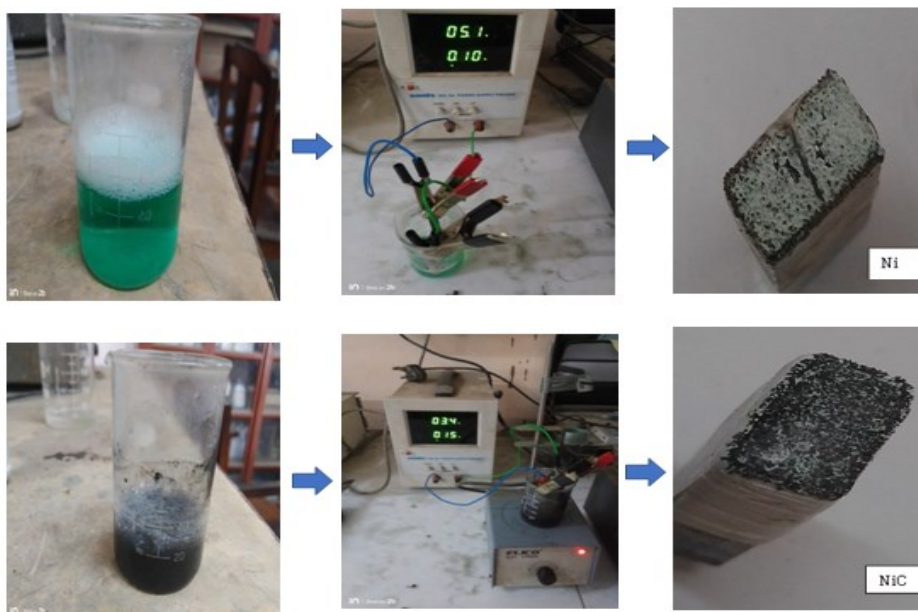


Fig. 3. Flowchart showing the development pathway of Ni and NiC materials

MnO₂ and MnO₂ with nanocarbon (Graphene) – The electrocatalytic coating was done on a stainless steel plate using the electrodeposition technique, as stated below. The steel samples were

first polished by emery papers 1/0 to 3/0 and then cleaned with acetone, and water. After cleaning, the coated samples were dried by hot air. A series of experiments were performed by varying the different parameters of the experiment, in order to find the optimum conditions (Table 3) of the electrodeposition process. After the coating, the sample was rinsed with ethanol and acetone and then dried at a temperature of 80°C for 6 hours. For MnO₂-graphene electrodeposition or coating, nanocarbon (graphene) in the powder form was used. The Steel sample was coated by a power supply machine (DC) using the same bath solution as mentioned above, along with the presence of suspended graphene powder, under similar electrodeposition conditions. All the electrodeposition parameters for the synthesis of MnO₂ and MnO₂C materials are tabulated in the below table.

Table 3. Showing the electrodeposition parameters for development of MnO₂ and MnO₂C electrocatalytic materials

Electroplating Parameters	Optimum Value (MnO ₂)	Optimum Value (MnO ₂ C)
MnSO ₄ : M	0.34	0.34
H ₂ SO ₄ : M	0.60	0.60
Nano carbon Powder : g/50ml	-----	2
Applied Current Density: mA/cm ²	260	200
Applied Potential : V	4.2	3.2
Time duration : minutes	10	15

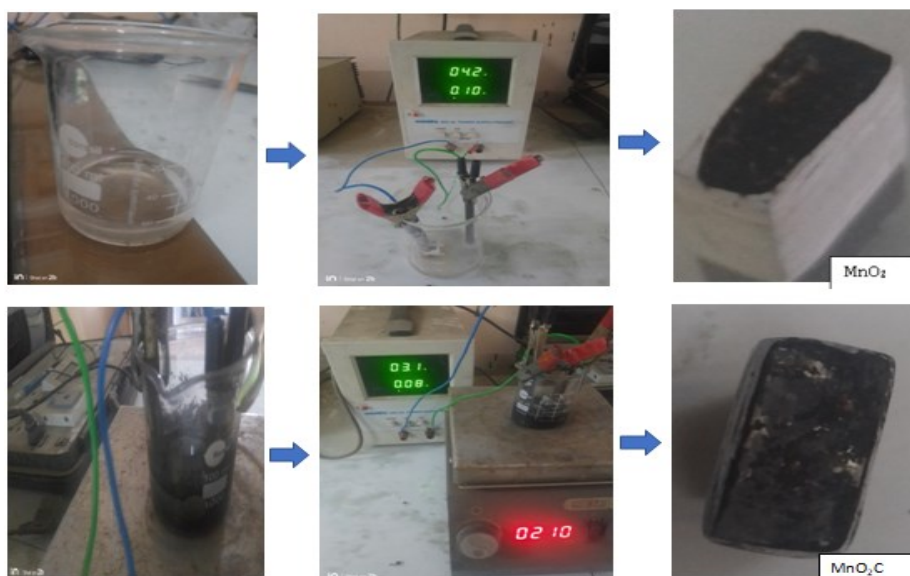


Fig. 4. Flowchart showing the development pathway of MnO₂ and MnO₂C

Various Electrochemical characterizations, such as CV, CA, PD, and EIS of the electrocatalytic surfaces synthesized were performed in the solution of SBF (Phosphate Buffer Solution with 200mg/dl glucose concentration) by a AUTOLAB potentiostat. The potentiostat was controlled by the NOVA 2.1.5 analyst software. All the electrochemical tests were carried out in a conventional three electrode cell system, having the developed electrocatalytic materials as the working electrode, a counter electrode (graphite rod) and a reference electrode (Saturated Calomel Electrode). The morphology of the developed structure of the electrode material was examined by Scanning Electron Microscopy (SEM) and the different phases developed in the electrode material were analyzed by X-Ray Diffraction (XRD).

Results and Discussions

Various electrochemical tests like Cyclic Voltammetry (CV), Electrochemical Impedance Spectroscopy (EIS), Chronoamperometry (CA), and Potentiodynamic Polarisation (PD) were performed with different electrocatalytic materials viz Platinum (Pt), Nickel (Ni), Nickel with nanocarbon (NiC), Manganese dioxide (MnO_2) and Manganese dioxide with nanocarbon (MnO_2C) in artificially made Simulated Body Fluid (SBF) with different concentrations of sugar, in accordance with diabetic patients worldwide. Material characterization of the developed electrodes was performed by Scanning Electron Microscopy (SEM) and Xray Diffraction (XRD) to find out the constituents of the developed material as well as their morphology.

Cyclic Voltammetry (CV)

Figure 5 shows the CV curves of the developed electrocatalytic materials in PBS solution containing 200mg/dl glucose. The test parameters for running the CV test are as follows.

Table 4. Test Parameters for running Cyclic Voltammetry (CV) test for the various electrocatalytic materials in SBF (Phosphate Buffer Solution with 200mg/dl glucose concentration)

Test Parameters	Value
Start Potential	-0.3 V wrt SCE
Upper Vertex Potential	1.5 V wrt SCE
Lower Vertex Potential	-0.5 V wrt SCE
Stop Potential	0.2 V wrt SCE
Scan Rate	100 mV/sec
Step	0.00244 V

The oxidation of glucose molecules electrochemically over the electrode (anode) surface is manifested by the increase in current (y-axis) at the onset voltage potential of about + 0.05V versus saturated calomel electrode (SCE). It is observed that the curves of all the four electrocatalytic materials are similar in nature, with a peak current density, which signifies the electrochemical oxidation rate of glucose, over the anode surface. The area enclosed by the curves signify the energy content of the fuel cell. It is worth noting that the electrode made with Ni-nanocarbon or graphene (Ni C) performs the best among all other electrodes. The maximum current density obtained is around 120 mA/cm², which is significant, i.e., an electrode with a surface area of around 10 cm² will generate 1.2 A. The electrochemical performance of MnO_2 -graphene(MnO_2C) is also decent, where the highest current density is around 60 mA/cm². It is also to be noted, that the energy obtained is enhanced when nanocarbon is added to either Ni or MnO_2 , in comparison to non-nanocarbon samples. The maximum current densities for all the developed electrocatalytic materials are tabulated in Table 5.

Table 5. Maximum current density values of different developed materials

Material	Max Current Density (mA/cm ²)
NiC	115
Ni	74
MnO_2C	59
MnO_2	17

Chronoamperometry

A steady current is produced by any stable electrocatalytic surface for a certain period of time before the surface becomes contaminated and gets less active electrochemically. Figure 6 shows the chronoamperometry (CA) graphs of all four developed materials, in the PBS solution containing 200mg/dl concentration. The applied potential is 1V wrt SCE, for 300 seconds. The results are like those obtained in the CV study. The steady-state current density has been enhanced

by the graphene and the material has become more energetic. Nickel Graphene electrode (NiC) is giving a steady state current of around 70 mA/cm^2 , which means an electrode with a 100 cm^2 surface area, can produce around 7 A of current in a glucose fuel cell, which is enough current for running small electric motors or other relevant devices without generating any pollutants.

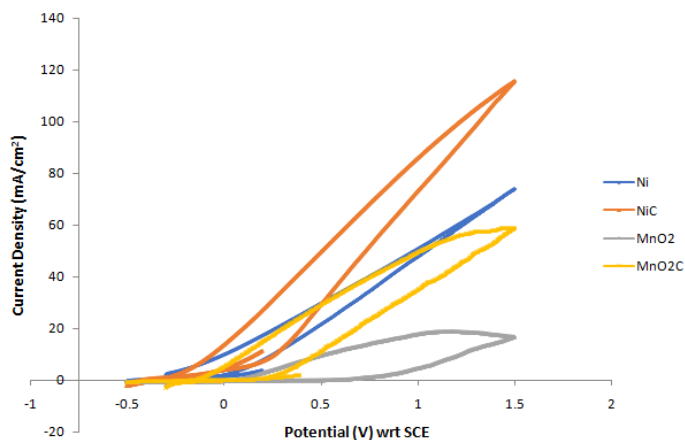


Fig. 5. Cyclic Voltammetry (CV) curves for the various electrocatalytic materials in SBF (Phosphate Buffer Solution with 200mg/dl glucose concentration)

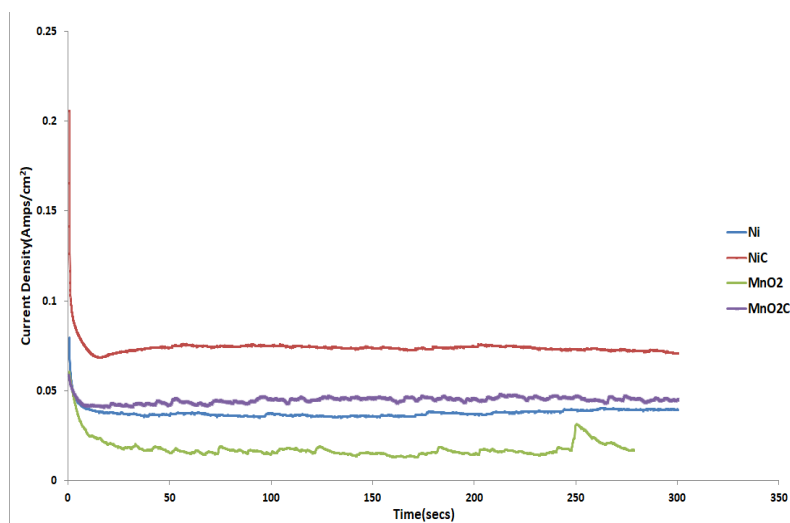


Fig. 6. Chronoamperometry (CA) curves for the various electrocatalytic materials in SBF (Phosphate Buffer Solution with 200mg/dl glucose concentration)

Potentiodynamic Polarisation

Fig. 7 depicts Potentiodynamic Polarisation curves for different electrocatalytic materials, with and without nanocarbon. The polarisation test was carried out from -1 V to $+1 \text{ V}$ wrt SCE potential window, at a scan rate of 5 mV/sec . The curve which shifts to the rightmost, produces max cell current density. It is seen, that the electrocatalytic material, Nickel with nanocarbon (NiC) produces max delivery current. It can be observed that the addition of surface-sensitive agents like graphene has increased the reversible cell current. The magnitude of the current can

be found by superimposing anodic and cathodic Tafel lines, as shown in the figure. It is seen that for the NiC electrode, the current is coming near about 1 mA/cm^2 , that is, an electrode of size of 1 inch by 1 inch, in a battery of 10 electrodes, can produce over 129 mA, which is enough current to run small electronic gadgets. Various parameters have been computed from the electrochemical test data, which are tabulated in Table 6.

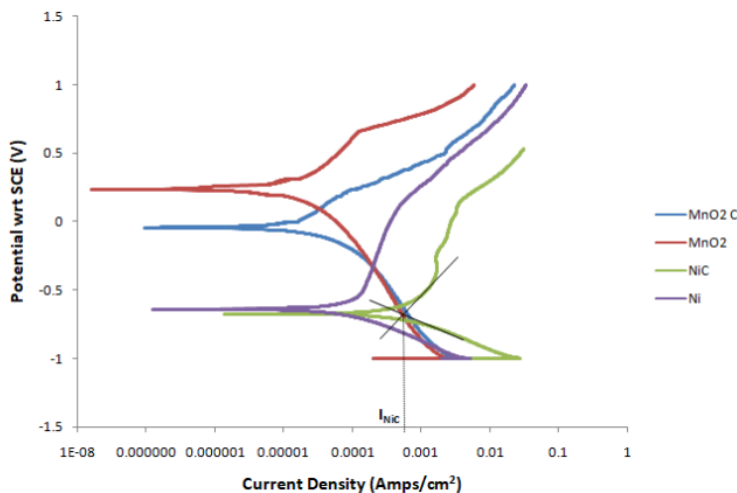


Fig. 7. Tafel Plots for the various electrocatalytic materials in SBF (Phosphate Buffer Solution with 200mg/dl glucose concentration)

Table 6. Various Parameters computed from the electrochemical test data of Potentiodynamic Polarisation

Material	Cell Current (mA/cm ²)	Cell Voltage (V)	β_{anodic} (mV/dec)	β_{Cathodic} (mV/dec)	Polarisation Resistance(Ω)
MnO ₂	0.003	0.240	109.93	104.28	14640
MnO ₂ C	0.008	-0.044	130.34	83.435	5918.40
Ni	0.104	-0.64	388.02	233.25	1219.40
NiC	0.920	-0.677	1107.1	248.47	191.72

Electrochemical Impedance Spectroscopy (EIS)

The electrochemical phenomenon that are happening at the electrolyte-metal interface can be studied by EIS and represented by the R-L-C circuit for an enhanced understanding of fundamental ideas of fuel oxidation on the electrocatalytic metal surface. In general, electrolyte-metal interface consists of layers of (+ve) charges and (-ve) charges, known as the electrical double layer, that produces either pseudo-capacitance or capacitance. Additionally, there are some resistance loads like Solution resistance (R_s) and Charge transfer resistance (R_p). There may also be more capacitance or induction due to coating. This phenomenon can be understood by Nyquist and Bode plots, as depicted below.

The electrochemical impedance spectroscopy test was done at frequencies from 1000 kHz and 0.1 Hz. Various parameters such as Charge transfer resistance (R_p), Solution resistance (R_s), constant phase element (CPE) or Capacitive load, and α are obtained from the EIS test (tabulated in table 7). α is obtained from the equation $Z = 1/C(j\omega)^{-\alpha}$.

Figure 8 shows the Nyquist plots for different electrocatalytic materials. The best-match EIS circuit is shown in the inset. It can be seen that the curves show a semicircle pattern (Randle circuit model). The semicircle diameter represents the Charge transfer resistance (R_p). Thus, as

the semicircle gets smaller, the R_p value gets lowered and thus the electrocatalytic property of the material gets enhanced. It can be observed that NiC electrocatalytic material shows the minimum diameter of the semicircle, which indicates it is a high electrocatalytic material, as far as the electrochemical conversion of sugar is concerned. This explains why the NiC electrocatalyst material has been observed to be the best energetic material, as seen in CV, PD, and CA figures (Figures 5–7). The Charge transfer resistance (R_p) value of NiC in this solution, is around 55 ohms.

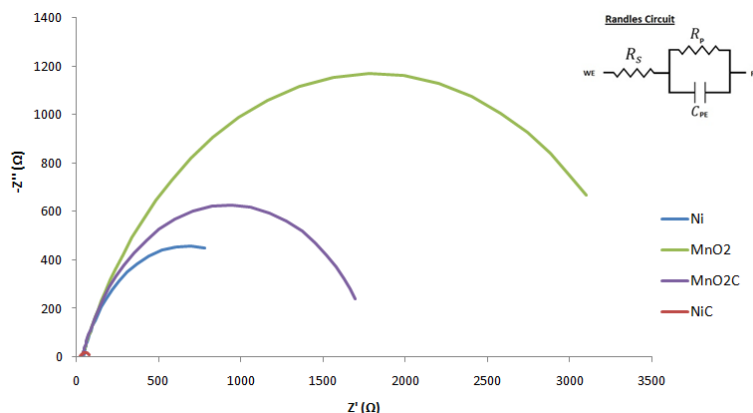


Fig. 8. Nyquist Plot for the various electrocatalytic materials in SBF (Phosphate Buffer Solution with 200mg/dl glucose concentration)

Table 7. Various parameters obtained from EIS test data

Material	Charge Transfer Resistance, R_p (Ω)	Solution Resistance, R_s (Ω)	Capacitive Load (μF)	α
NiC	54.969	23.64	3491.8	0.704
Ni	1267.4	40.58	777.76	0.797
MnO ₂ C	1783.8	35.937	84.248	0.779
MnO ₂	3986.7	21.854	87	0.742

Electrochemical Impedance Spectroscopy data is also analyzed by Bode plots (Figs. 9 and 10), and they indicate two parameters: the phase angle shift and the impedance. The Bode Plot in figure 9 shows the impedance values for the various electrocatalytic materials. The impedance is measured by the gap between the higher and lower ordinates (Z) of a particular curve. The Bode Curve also agrees with the result obtained in the Nyquist Plot. It is seen that the y value or the impedance value of Nickel with nanocarbon (NiC) is minimum (100 ohms), indicating highly energetic material.

Fig. 10 shows the Bode Plot (phase angle). If there is an angle shift towards -90° , it shows the presence of a capacitive load. If the shift in the phase angle is lesser than 90° , then a pseudo capacitance may be there, i.e., the electrochemical system works like a capacitive load, however the capacitance is not pure. As can be observed from Fig. 10, for all the electrodes the phase angle shifts towards -60° at a certain frequency range (1-100 Hz), which indicates an R–L–C circuit having a capacitive load; however, it is a pseudo capacitance, not a pure one. The value of α less than 1 for all the electrocatalytic materials also indicates that actually, pseudo capacitance exists in the R–L–C circuit for all the electrode systems.

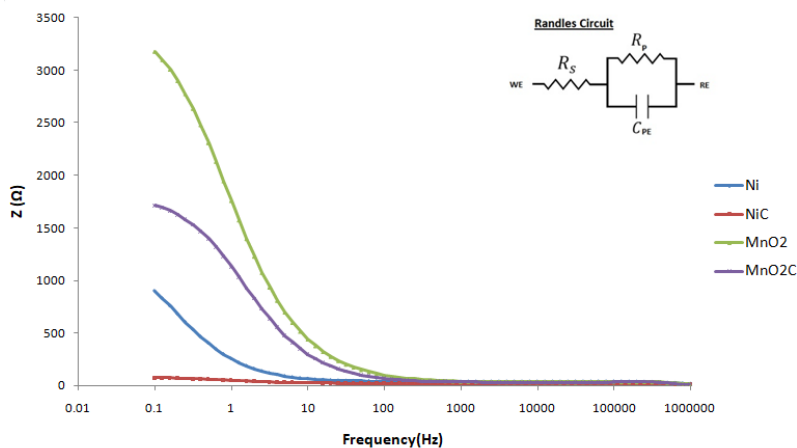


Fig. 9. Bode Plot (impedance) for the various electrocatalytic materials in SFB (Phosphate Buffer Solution with 200mg/dl glucose concentration)

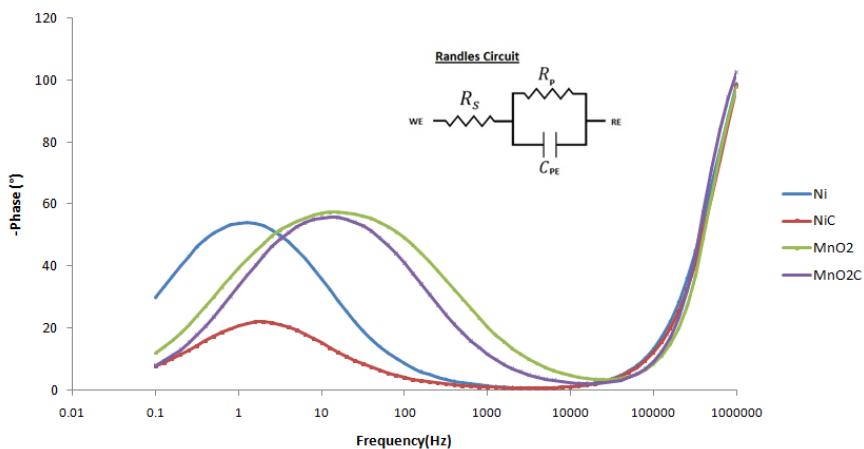


Fig. 10. Bode Plot (phase angle) for the various electrocatalytic materials in SFB (Phosphate Buffer Solution Solution with 200mg/dl glucose concentration)

X-ray Diffraction (XRD)

XRD analysis was done by Rigaku Ultima III diffractometer, in the 2 theta range of 20° to 80°. Fig. 11 shows the XRD pattern of electrodeposited Nickel nanocarbon (Ni C) material, on SS substrate. It shows the peak intensity at different 2 theta values. The bigger peaks are from Ni and nanocarbon phases. Similarly, Fig. 12 shows the XRD pattern of electrodeposited MnO₂ with nanocarbon, on SS substrate. The relatively smaller peaks represent the constituents of the SS substrate (which are of no interest for the present research). This confirms electrodeposition of Ni with nanocarbon, and MnO₂ with nanocarbon, on SS substrate.

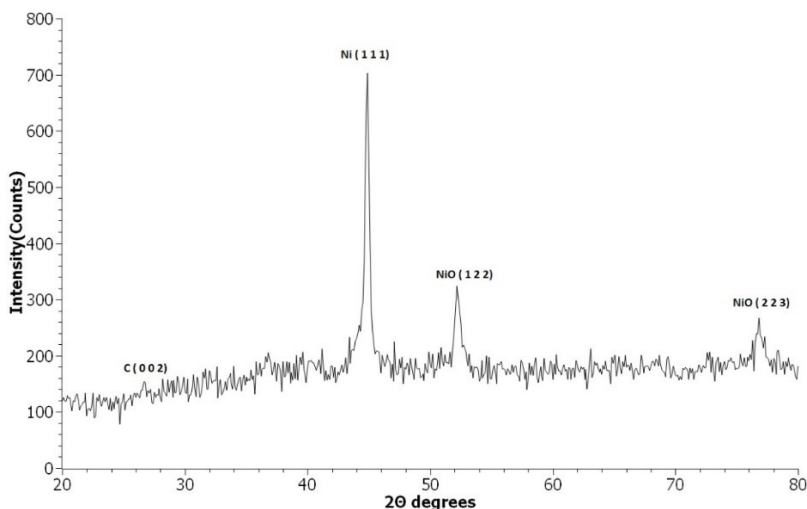


Fig. 11. XRD pattern of developed material NiC

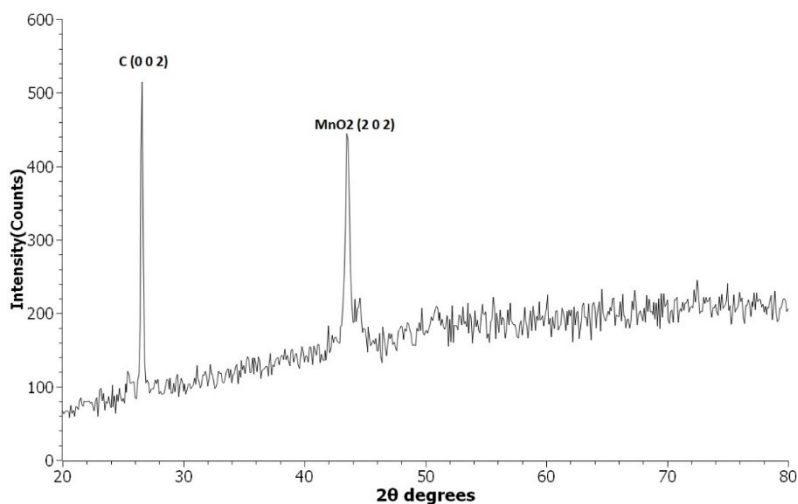


Fig. 12. XRD pattern of developed material MnO₂C

Scanning Electron Microscopy (SEM)

The morphologies of the developed electrocatalytic materials, Nickel with nanocarbon (NiC) and Manganese dioxide with nanocarbon (MnO₂C) were examined under SEM. SEM image morphology is shown in Fig. 13. The NiC material (Fig. 13A) shows a 3Dimensional microscopic structure having a relatively high surface-to-volume ratio. The images show an enhanced electrocatalytic surface area with 3D features available for the fuel to get electrochemically oxidized, which produces higher current, which was found in the electrochemical characterization. It is worth noting that the nano Carbon particles' distribution was random within the Nickel matrix. The morphology of the MnO₂C material (Fig. 13B) exhibits an effective more 3D space on which electrochemical oxidation of glucose has taken place. This increase in the effective surface area accounts for the higher current, being delivered from the oxidation of glucose.

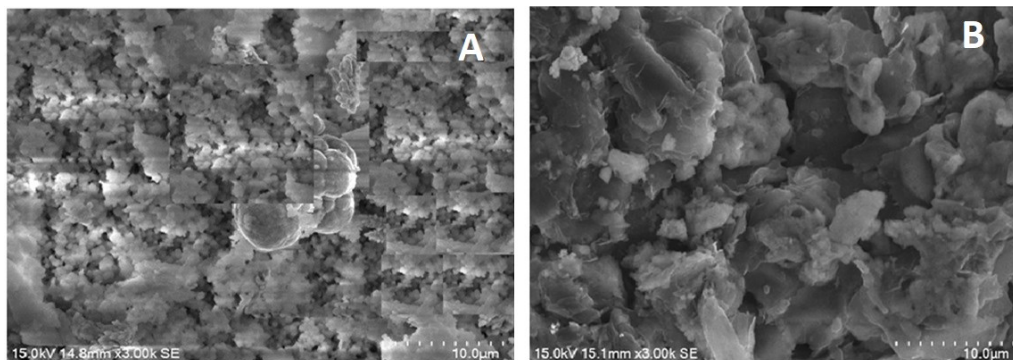


Fig. 13. SEM image of: a) NiC at x3000 magnification; b) MnO₂C at x3000 magnification

Sugar Level Detection System

Platinum electrodes have been extensively used in electrochemical sensors to detect glucose levels [24-27]. In order to detect the sugar level in SBF solution, Calibration curves were used. These curves were obtained by running CV tests in SBF solutions with 6 different sugar levels, starting from 0 mg/dl sugar level, up to 300 mg/dl. AUTOLAB potentiostat was used for this test, with Platinum and Graphite Rod as the Working Electrode and Counter Electrode respectively. It was observed that the peak current density value obtained from a particular CV test, was directly proportional to the sugar level in the solution, as can be seen the Fig. 14. A linear regression analysis (Fig. 15) was done on this data, which gave a linear equation between the sugar level and the corresponding peak current value. The coefficient of determination (R^2) value of this analysis came out to be 0.974, i.e., the linear relationship between the sugar level and the corresponding peak current density value, was about 97.4% accurate. This linear equation was used to find out any unknown sugar level in SBF solution, by running a CV test and putting the corresponding peak current density value, in the equation.

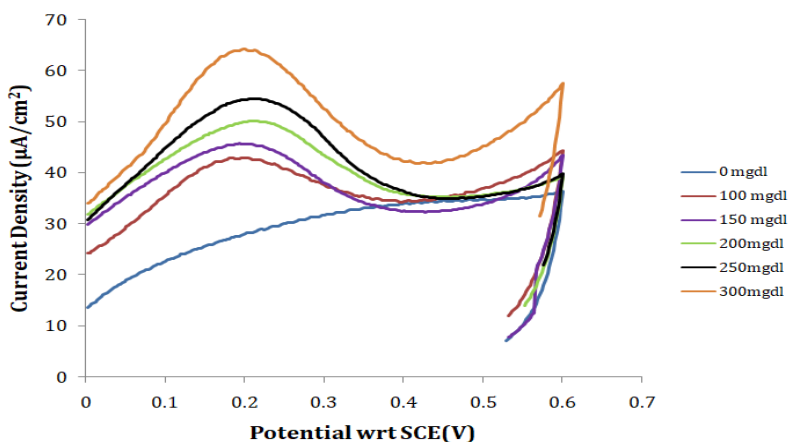


Fig. 14. Calibration Curves showing different peak current density values for different glucose concentrations for detection of glucose concentration in SBF (Phosphate Buffer Solution with 0.01M NaOH)

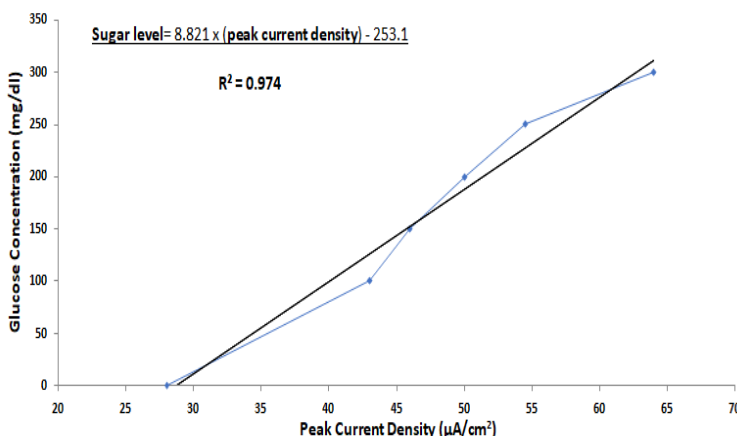


Fig. 15. Linear Regression Plot showing linear relationship of glucose concentration with peak current densities, with the linear regression equation

Electro-oxidation of excess sugar in SBF

Electro-oxidation of excess sugar in SBF solution was carried out by running CA and CV procedures, over platinum and the various developed materials respectively. The CA procedures were run at 0.25V vs SCE, for 60 seconds. The parameters of the CV procedures are tabulated in Table no 8.

Table 8. Test Parameters for CV test, to electro-oxidize 200 mg/dl glucose in SBF (PBS solution with 0.01M NaOH) by various electrocatalytic electrode materials

Test Parameters	Value
Start Potential	0 V wrt SCE
Upper Vertex Potential	1 V wrt SCE
Lower Vertex Potential	0 V wrt SCE
Stop Potential	0.5 V wrt SCE
Number of scans	5
Scan Rate	100 mV/sec
Step	0.00244 V

After running these procedures, the sugar levels were measured using the linear regression model, and from that the reduction in sugar levels was found, and the corresponding energy was released. The below tables (table no. 9 and no. 10) show the detailed results of the electro-oxidation of excess sugar. The energy released is obtained by multiplying the difference of the peak current densities before and after CA/CV, with the potential value (0.2V) at which the peak current is occurring (from Figure 14).

Table 9. Data regarding the lowering of glucose level by Pt electrode in SBF (PBS solution with 0.01M NaOH) and corresponding energy released

Glucose Level (mg/dl)	Glucose Level after CA (mg/dl)	Peak Current Density (µA/cm²)	Peak Current Density after CA (µA/cm²)	Energy released (µWatt/cm²)
250	152.67	57.04	46	2.21
200	130.61	51.37	43.5	1.57
150	112.97	45.70	41.5	0.84

Table 10. Data regarding lowering of glucose level by different electrodes in SBF (200 mg/dl glucose in PBS solution with 0.01M NaOH) and corresponding energy released

Electrode	Glucose Level after CV (mg/dl)	Peak Current Density ($\mu\text{A}/\text{cm}^2$)	Peak Current Density after CV ($\mu\text{A}/\text{cm}^2$)	Energy released ($\mu\text{Watt}/\text{cm}^2$)
NiC	51.22	51.37	34.5	3.374
Ni	90.92	51.37	39	2.474
MnO ₂ C	99.74	51.37	40	2.274
MnO ₂	152.67	51.37	46	1.074

Conclusions

Different electrocatalytic materials 1) Nickel 2) Nickel with nanocarbon 3) Manganese dioxide (MnO₂) and 4) Manganese dioxide with nanocarbon (MnO₂C), were developed by electrodeposition process and subsequently electrochemically tested and microscopically characterized. Excellent electrochemical performances were observed. Direct linear relationship between blood sugar level and peak current density was established over Platinum working electrode, with over 97% accuracy. Different electrocatalytic materials as working electrodes were successful in lowering the sugar level in SBF solution, by electro-oxidizing.

Acknowledgement

We acknowledge the support of the Lab in Charge of the X-ray & Metal Physics Laboratory and Chemical Analysis Laboratory, at the Department of Metallurgical and Material Engineering, Jadavpur University, where the material characterizations were done.

References

- [1] *Diabetes Mellitus (DM) - Hormonal and Metabolic Disorders*, <https://www.msmanuals.com/home/hormonal-and-metabolic-disorders/diabetes-mellitus-dm-and-disorders-of-blood-sugar-metabolism/diabetes-mellitus-dm>, Retrieved 1 October 2022.
- [2] *Diabetes*, https://www.who.int/health-topics/diabetes#tab=tab_1, Retrieved 29 January 2023.
- [3] A.E. Kitabchi, G.E. Umpierrez, J.M. Miles, J.N. Fisher, *Hyperglycemic crises in adult patients with diabetes*, **Diabetes Care**, **32**, 2009, p. 1335, <https://doi.org/10.2337/dc09-9032>.
- [4] Kharroubi AT, Darwish HM, *Diabetes mellitus: The epidemic of the century*, **World J Diabetes**, **6**, 2015, pp. 850-867, <https://doi.org/10.4239/wjd.v6.i6.850>.
- [5] K. Maheshwari, Karishma, S. Sharma, A. Sharma, S. Verma, *Fuel Cell and Its Applications: A Review*, **International Journal of Engineering Research & Technology**, **7**, 2018, pp. 6-9.
- [6] S. Paul, A. Ghosh, *Electrochemical Characterization of MnO₂ as Electrocatalytic Energy Material for Fuel Cell Electrode*, **The Journal of Fuel Chemistry and Technology**, **43**, 2015, pp. 344–351, [https://doi.org/10.1016/S1872-5813\(15\)30008-6](https://doi.org/10.1016/S1872-5813(15)30008-6).
- [7] S. Paul and Ruma Chatterjee, *Development of Nano Carbon-MnO₂ Energy Material for Glucose Fuel Cell Electrode*, **Nanomaterials and Energy**, **3**, 2015, pp. 1–9, <https://doi.org/10.1680/nme.14.00030>.
- [8] S. Paul and A. Ghosh, *MnO₂, A High Electrocatalytic Energy Material to Synthesis Energy from Oxidation of Methanol in Fuel Cell*, **Energy and Environment Focus**, **5**, 2015, pp. 1–7, <https://doi.org/10.1166/eef.2016.1184>.
- [9] S. Guchhait and S. Paul, *Synthesis and Characterization of ZnO-Al₂O₃ Oxides as Energetic Electrocatalytic Material for Glucose Fuel Cell*, **The Journal of Fuel Chemistry and Technology**, **43**, 2015, pp. 1004–1010, [https://doi.org/10.1016/S1872-5813\(15\)30029-3](https://doi.org/10.1016/S1872-5813(15)30029-3).

- [10] S. Paul, S.K. Naimuddin, A. Ghosh, *Electrochemical Characterization of Ni-Co and Ni-Co-Fe for Oxidation of Methyl Alcohol Fuel with High Energetic Catalytic Surface*, **The Journal of Fuel Chemistry and Technology**, **42**, 2014, pp. 87–95, [https://doi.org/10.1016/S1872-5813\(14\)60012-8](https://doi.org/10.1016/S1872-5813(14)60012-8).
- [11] S. Paul and S.K. Naimuddin, *Electrochemical Characterization of Synthesized Ni-Co and Ni-Co-Fe Electrodes for Methanol Fuel Cell*, **The Journal of Fuel Cell Science and Technology**, **11**, 2014, pp. 18–25, [https://doi.org/10.1016/S1872-5813\(14\)60012-8](https://doi.org/10.1016/S1872-5813(14)60012-8).
- [12] S. Paul, *Materials and Electrochemistry: Present and Future Battery*, **Journal of Electrochemical Science and Technology**, **7**, 2016, pp. 115-131 <https://doi.org/10.5229/JECST.2016.7.2.115>.
- [13] S. Paul, *Electrochemical Energy Synthesis and Storage in Battery and Fuel Cell*, Amazon Pub, India, 2016, pp. 82–112, ISBN -13: 978-1520321929.
- [14] S. Paul, AK Mondal, *Development of graphene–Ni–NiO energetic catalytic materials for electrochemical energy*, **Nanomaterials and Energy**, **9**, 2020, pp. 1-7, <https://doi.org/10.1680/jnaen.19.00054>.
- [15] S. Paul, A. Paria, *Development of NiO-Nanocarbon and MnO₂-Nanocarbon Energetic Catalytic Electrode Materials to Synthesize Electrical Energy through Electrochemical Oxidation of Glucose*. **Journal of Materials Engineering and Performance**, 2019 <https://doi.org/10.1007/s11665-019-04138-4>.
- [16] B. Yu, B. Vassilyev, O.A. Khazova, N.N. Nikolaeva, *Kinetics and mechanism of glucose electrooxidation on different electrode-catalysts: Part I. Adsorption and oxidation on platinum*, **Journal of Electroanalytical Chemistry and Interfacial Electrochemistry** **196**, 1985, pp. 105-125, [https://doi.org/10.1016/0022-0728\(85\)85084-1](https://doi.org/10.1016/0022-0728(85)85084-1).
- [17] T.W. Tsai, G. Heckert, L.F. Neves, Y.Q. Tan, D.Y. Kao, R.G. Harrison, D.E. Resasco, D.W. Schmidtke, *Adsorption of glucose oxidase onto single-walled carbon nanotubes and its application in layer-by-layer biosensors*, **Analytical Chemistry**, **81**, 2009, pp. 7917–7925, <https://doi.org/10.1021/ac900650r>.
- [18] F.Q. Tang, X.W. Meng, D. Chen, J.G. Ran, C.Q. Zheng, *Glucose biosensor enhanced by nanoparticles*, **Science China B**, **43**, 2000, pp. 268–274, <https://doi.org/10.1007/BF02969521>.
- [19] Y. Degani, A. Heller, *Electrical communication between redox centers of glucose oxidase and electrodes via electrostatically and covalently bound redox polymers*, **Journal of the American Chemical Society**, **111**, 1989, pp. 2357–2358, <https://doi.org/10.1021/ja00188a091>.
- [20] W. Loeb, *Sugar decomposition III. Electrolysis of dextrose*, **Biochemische Zeitschrift**, **17**, 1909, pp. 132–144.
- [21] J. Chen, W.D. Zhang, J.S. Ye, *Nonenzymatic electrochemical glucose sensor based on MnO₂/MWNTs nanocomposite*, **Electrochemistry Communications**, **10**, 2008, pp. 1268–1271, <https://doi.org/10.1016/j.elecom.2008.06.022>.
- [22] A. Khan, A.A.P. Khan, H.M. Marwani, M.M. Alotaibi, A.M. Asiri, A. Manikandan, S. Siengchin, S.M. Rangappa, *Sensitive Non-Enzymatic Glucose Electrochemical Sensor Based on Electrochemically Synthesized PANI/Bimetallic Oxide Composite*, **Polymers**, **14**, 2022, p. 3047, <https://doi.org/10.3390/polym14153047>.
- [23] *Phosphate-Buffered Saline or PBS Solution*, <https://www.thoughtco.com/phosphate-buffered-saline-pbs-solution-4061933>, Retrieved Apr 5, 2023.
- [24] J.H. Shim, K.Y. Jang, C. Lee, Y. Lee, *Applications of porous Pt-filled micropore electrode: direct amperometric glucose detection and potentiometric pH sensing*, **Electroanalysis**, **23**, 2011, pp. 2063– 2069.
- [25] S.Y. Joo, S.J. Park, T.D. Chung, H.C. Kim, *Integration of a nanoporous platinum thin film into a microfluidic system for non-enzymatic electrochemical glucose sensing*, **Analytical Sciences**, **23**, 2007, pp. 277–2.

- [26] M.Q. Guo, H.S. Hong, X.N. Tang, H.D. Fang, X.H. Xu, *Ultrasonic electrodeposition of platinum nanoflowers and their application in nonenzymatic glucose sensors*, **Electrochimica Acta**, **63**, 2012, pp. 1–8.
- [27] T. Unmüssiga, A. Weltin, S. Urban, P. Daubinger, G. A. Urban, J. Kieninger, *Non-enzymatic glucose sensing based on hierarchical platinum micro-/ nanostructures*, **Journal of Electroanalytical Chemistry**, **816**, 2018, pp. 215-222, <https://doi.org/10.1016/j.jelechem.2018.03.061>.
-

Received: January 28, 2024

Accepted: February 02, 2024